

Gravitational waves in a flat radiation–matter universe including anisotropic stress

Andrew J. Wren,^{1,*} Jorge L. Fuentes,^{1,†} and Karim A. Malik^{1,‡}

¹*Astronomy Unit, School of Physics and Astronomy,
Queen Mary University of London, Mile End Road, London, E1 4NS, United Kingdom*

(Dated: May 9, 2022)

We present novel analytical solutions for linear–order gravitational waves or tensor perturbations in a flat Friedmann–Robertson–Walker universe containing two perfect fluids, radiation and pressureless dust, and allowing for neutrino anisotropic stress. One of the results is applicable to any sub–horizon gravitational wave in such a universe. Another result is applicable to gravitational waves of primordial origin, for example produced during inflation, and works both before and after they cross the horizon. These results improve on analytical approximations previously set out in the literature. Comparison with numerical solutions shows that both these approximations are accurate to within 1%, or better, for a wide range of wave–numbers relevant for cosmology.

PACS numbers: 02.30.Hq, 02.30.Mv, 02.60.Gf, 04.25.Nx, 04.30.Tv, 95.35.+d, 95.30.Sf, 98.80.-k, 98.80.Cq, 98.80.Jk

I. INTRODUCTION

In 2016 observations by LIGO [1] have directly detected gravitational waves for the first time. The origin of these waves was astrophysical: the merger of two large stellar mass black holes. In contrast, primordial gravitational waves originating from inflation have been constrained, but not detected, by for example PLANCK satellite observations, combined with data from BICEP2/Keck Array [2] and with other data sources [3]. The simplest inflationary models consistent with these results tend to favour inflationary scenarios which generate gravitational waves of relatively low, but non–negligible, amplitude compared with scalar perturbations.

In this paper we consider gravitational waves with sufficiently small amplitude to be modelled as linear tensor perturbations travelling through a flat Friedmann–Robertson–Walker (FRW) universe filled with radiation and matter. The matter component is pressureless dust, and our perturbation equations treat both radiation and matter as perfect fluids. We allow for a source term due to neutrino anisotropic stress.

As recalled in for example Refs. [4–12], there are well known exact analytical expressions for the evolution of linear tensor perturbations in a flat universe dominated by either radiation only or matter (pressureless dust) only. These approximations do not work particularly well when used for a universe containing both radiation and matter. The next simplest approximation is to use the radiation–only solution before the time of radiation–matter equality, and the matter–only solution after that time. A slightly more sophisticated approach, used for example in Refs. [5, 6], is to match these two solutions together at the time of radiation–matter equality, termed the “sudden approximation”. Reference [6] shows that these approaches do not provide particularly good approximations to a numerical solution of the linear tensor perturbation equation. In Ref. [7], a smoother transition is sought between the radiation and matter solutions, fitting parameters to numerical solutions, a method which is most suited to dealing with wave–numbers much lower (corresponding to much larger wave–lengths) than those we consider.

Later work in Refs. [8–12] is aimed primarily approximating the effects of neutrino free–streaming as expressed via an integro–differential equation derived in Refs. [8, 13], rather than at improving accuracy in the perfect fluid model of radiation and matter. In this paper we are improving the accuracy of the solutions also in the case of non-zero anisotropic stress.

We now briefly survey the accuracy of the approximations of Refs. [6, 9–12]. References [6, 9], Ref. [11] and Ref. [10] pursue three different forms of the Wentzel–Kramers–Brillouin (WKB) method for finding approximate analytical solutions for ordinary differential equations.

*andrew.wren@ntlworld.com

†j.fuentesvenegas@qmul.ac.uk

‡k.malik@qmul.ac.uk

The methods of Refs. [6, 9] and Ref. [11] provide results which, when restricted to the perfect fluid case, are accurate for primordial gravitational waves to within about 10% for inverse wave-numbers, evaluated at the present day, of around 10–15 Mpc. Reference [10] presents another form of WKB approximation for a flat radiation–matter universe. Restricted to the perfect fluid case, this provides a good sub–horizon approximation for gravitational waves of primordial origin. However, it does not retain such good accuracy outside the horizon, and covers only one of the two independent solutions of the governing equation for tensor perturbations.

A different kind of approach is pursued in Ref. [12], using sums of spherical Bessel functions of successive orders to approximate tensor perturbations. However, Ref. [12]’s approach is best used for numerical calculations based on expansions of very high order — they exemplify solutions to 20th and 100th order.

We derive improved results by employing a method set out, in a non–cosmological context, by Feshchenko, Shkil’ and Nikolenko (FSN) in 1966 [14], and used by two of the authors in a recent paper [15] to approximate the solutions of the ordinary differential equations governing scalar density perturbations. The FSN method is well suited for solving linear second order ordinary differential equations, that also depend on a small parameter, which here we take to be the inverse wave–number. In effect, this approach extends the WKB method of Ref. [11].

Following this introduction, in Section II of this paper, we recall the differential equation which governs tensor metric perturbations, focusing on a flat radiation–matter universe, and also noting the simpler differential equation for a flat radiation–only model and its analytical solution with and without neutrino anisotropic stress. In Section IV A, we then use the method first set out in Ref. [14] to find an approximate analytical solution to the governing equation of Section II. Because tensor perturbations are governed by only a single second order differential equation, application of the method in this paper is more straightforward than the work of Ref. [15] on scalar perturbations where a set of coupled differential equations is involved¹.

Our approximation method is based on the *sub–horizon* assumption that the tensor perturbation has a wave–number larger than the Hubble parameter. However, using numerical solutions, we can see that, for a wide range of wave–numbers, it is possible to extend the approximation back to earlier times when the wave–number is similar to the Hubble parameter. We find the approximation of third order in the inverse wave–number is accurate to within 1% or better for gravitational waves with a present day inverse wave–number less than, or equal to, around 17 Mpc.

Section V extends the analytical approximation to cover gravitational waves of primordial origin, from early times when their wave–length is larger than the horizon through their subsequent sub–horizon evolution. Our approximation to second order in the inverse wave–number accurate to within 1%, or better, for gravitational waves corresponding to those with an actual present day inverse wave–number less than, or equal to, around 35 Mpc. This range includes wave–numbers which represent scales of key relevance for structure formation in the Universe, and broadly corresponds to CMB multipoles $l \gtrsim 120$.

Section VI concludes the paper. It summarises the results and provides a brief discussion.

A *Mathematica* notebook which executes the approximation method automatically is available online at Ref. [16]. It enables all the approximations presented in this paper to be calculated in less than a second on a standard PC. The template can be easily adapted for use with other, similar, second order differential equations.

Throughout this paper, we work in conformal time τ , with a dash indicating the derivative of a function with respect to conformal time. We set the speed of light $c = 1$, co–moving spatial co–ordinates are denoted x^i and Latin indices i, j, k range from 1 to 3.

II. LINEAR TENSOR PERTURBATIONS

We now study linear perturbations in a flat Friedmann–Robertson–Walker (FRW) model with two non–interacting perfect fluids — radiation and matter, the latter being pressureless dust. We begin with the background equations, with the conformal time Friedmann equation for such a model being given by

$$\mathcal{H}^2 = \frac{8\pi G}{3} a^2 (\rho_r + \rho_m), \quad (2.1)$$

¹ The scalar perturbations of Ref. [15] depend on a pair of second order differential equations to determine the radiation density and metric perturbations, plus an additional second order differential equation to get the matter density perturbation.

where \mathcal{H} is the conformal Hubble factor, G is the gravitational constant, a is the scale factor, ρ_r the homogeneous radiation density, and ρ_m the homogeneous matter density. As usual, the radiation and matter densities obey

$$\rho_r \propto a^{-4} \quad \text{and} \quad \rho_m \propto a^{-3}, \quad (2.2)$$

and, as noted in, for example, Refs. [15, 17], the scale factor is given by

$$a(\tau) = a_{\text{eq}} \left(\frac{\tau}{\tau_c} + \frac{\tau^2}{4\tau_c^2} \right), \quad (2.3)$$

where a_{eq} is the time of radiation–matter equality, τ is the conformal time, and $\tau_c = \sqrt{2}/\mathcal{H}_{\text{eq}}$. In the following, we will use a normalised conformal time co–ordinate and replace τ/τ_c by τ , giving us the simpler expression

$$a(\tau) = a_{\text{eq}} \left(\tau + \frac{\tau^2}{4} \right). \quad (2.4)$$

We also normalise the co–moving wave–number k by using the corresponding inverse units $\tau_c^{-1} = \mathcal{H}_{\text{eq}}/\sqrt{2}$, and we note that, in those units, the conformal Hubble parameter is then given by

$$\mathcal{H}(\tau) = \frac{2(2 + \tau)}{\tau(4 + \tau)}. \quad (2.5)$$

For future reference, using the cosmological parameters of Ref. [3], we find that we have

$$\mathcal{H}_{\text{eq}}/\sqrt{2} = 0.00727 a_0 \text{ Mpc}^{-1}, \quad (2.6)$$

where a_0 is the value of the scale factor at the present time, *assuming the universe contains only radiation and matter*. To compare inverse wave–numbers with *actual* present day distances, we use a value of a_0 which takes account of the expansion of the Universe due to dark energy. From for example Ref. [18], we find that the Universe is currently some 16% bigger than it would have been without dark energy. If, as used implicitly in Ref. [3], we take the actual present day value of a_0 to be 1, then, in the universe with only radiation and matter assumed in Eq. (2.6) we have $a_0 \approx 1/1.16 \approx 0.86$, giving us

$$\mathcal{H}_{\text{eq}}/\sqrt{2} = 0.0063 \text{ Mpc}^{-1}. \quad (2.7)$$

For use below, in drawing figures directly comparable with those of Ref. [9], we note the conformal time of recombination, τ_r . Using the redshift of $z_* = 1089.90$ from [3], we find $\tau_r = 2.56069$.

To describe perturbations about this model, we follow the formalism of for example Ref. [19], and allow linear perturbations to the metric. To linear order, tensor, vector and scalar perturbations decouple. We therefore can focus solely on tensor perturbations and the metric then has a line element

$$ds^2 = a^2 \left(-d\tau^2 + [\delta_{ij} + h_{ij}] dx^i dx^j \right), \quad (2.8)$$

where h_{ij} are transverse, traceless metric tensor perturbations which depend on both τ and the co–moving spatial co–ordinate \mathbf{x} . At this linear order, transverse, traceless tensor perturbations do not depend on any choice of gauge.

The tensor perturbations have two independent polarisations, $+$ and \times ,

$$h_{ij}^+ = h^+ e_{ij}^+ \quad \text{and} \quad h_{ij}^\times = h^\times e_{ij}^\times, \quad (2.9)$$

where the polarisation matrices e_{ij}^+ and e_{ij}^\times represent eigenmodes of the spatial Laplacian, each satisfying

$$\nabla^2 e_{ij} = -k^2 e_{ij}, \quad (2.10)$$

and the Laplacian's derivatives are with respect to the co–moving co–ordinate \mathbf{x} , with k being the perturbation's co–moving wave–number.

The governing equation for the tensor perturbations with neutrino anisotropic stress is given, in general, by (see e.g. MalikWands, Rebhan)

$$h_{ij}''(\tau) + 2\mathcal{H}h_{ij}'(\tau) + \nabla^2 h_{ij}(\tau) = 16\pi G \pi_{ij}^{(\nu)}, \quad (2.11)$$

where $\pi_{ij}^{(\nu)}$ denotes neutrino anisotropic stress, which obeys the constraints

$$\pi_i^i = 0, \quad \text{and} \quad \partial_i \pi_{ij} = 0. \quad (2.12)$$

For a perfect fluid $\pi_{ij} = 0$, but this is not true in general.

III. GOVERNING EQUATIONS

We can now rewrite the general evolution equation for the tensor perturbations, Eq. (2.11) above, for the particular cases we would like to find solutions. We start with simplest case, in which the anisotropic stress is vanishing.

A. Perfect fluid

1. Radiation and dust

As set out in, for example, Ref. [19], for a model where the energy density is in the form of perfect fluids, the tensor perturbation parameters, h^+ and h^\times , from Eq. (2.9) each are separately governed by the conformal time equation

$$h''(\tau) + 2\mathcal{H}h'(\tau) + k^2h(\tau) = 0, \quad (3.1)$$

where \mathcal{H} is again the conformal Hubble parameter and the dashes denote differentiation with respect to τ . Using Eq. (2.5), we can therefore write Eq. (3.1) explicitly in terms of τ as

$$h''(\tau) + \frac{4(2+\tau)}{\tau(4+\tau)}h'(\tau) + k^2h(\tau) = 0. \quad (3.2)$$

This is the governing equation for linear tensor perturbations in a flat universe filled with radiation and pressureless matter, without a cosmological constant, and with no source term due to anisotropic stress.

2. Radiation only

Similarly, we can derive the governing equation for linear tensor perturbations in flat universes which contain either only radiation or only matter. Unlike, Eq. (3.2), the governing equations in each of these simpler models has tractable, and well known, analytical solutions.

For example, with only radiation, the Friedmann equation can be solved to show that $a \propto \tau$. We then have $\mathcal{H} = 1/\tau$, giving us the governing equation for our perturbation, h_r , as

$$h_r''(\tau) + \frac{2}{\tau}h_r'(\tau) + k^2h_r(\tau) = 0. \quad (3.3)$$

As recalled in, for example, Refs. [4–7, 9, 10], it is well-known that this can easily be solved analytically to give h_r as a linear combination

$$h_r(\tau) = A_s \frac{\sin(k\tau)}{k\tau} + A_c \frac{\cos(k\tau)}{k\tau}, \quad (3.4)$$

where A_s and A_c are real constants set by initial conditions.

This solution also describes the evolution of gravitational waves which originate very early in the history of a flat radiation–matter universe, when the matter density can be neglected relative to the radiation density. Any primordial A_c component may be neglected because it decays very rapidly in early times, as can be seen from Figure 1. In Section V, we will use this property to allow us to neglect the A_c component for gravitational waves which have a very early cosmological origin, such as inflation.

For use in the following sections, we recall that a perturbation with wave-number k is said to cross the horizon at the time τ_k when $\mathcal{H} = k$. From Eq. (2.5) we get

$$\tau_k = \frac{\sqrt{4k^2 + 1} - 2k + 1}{k} = \frac{1}{k} + \mathcal{O}\left(\frac{1}{k^2}\right), \quad (3.5)$$

where the $\mathcal{O}(1/k^2)$ means that the remaining part of the expression is of order $1/k^2$.

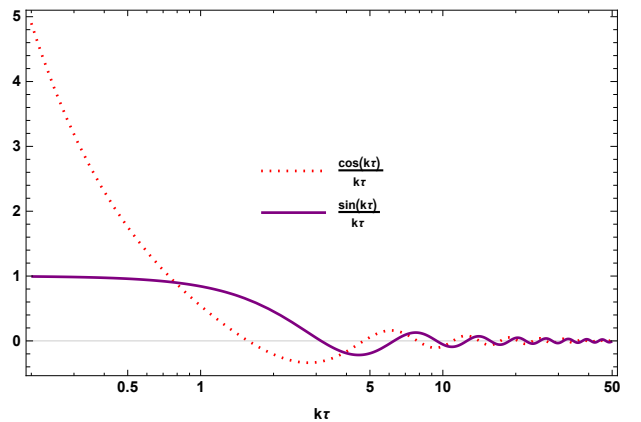


FIG. 1: Components of the analytical solution for linear tensor perturbations in a flat radiation–only universe, as set out in Eq. (3.4) for a perfect fluid. The $k\tau$ axis is logarithmic.

B. Including anisotropic stress

1. Radiation and dust, including anisotropic stress

From III A 2 we have an analytical solution for the tensor perturbations in a perfect fluid. Here we denote how we can extend this to include neutrino anisotropic stress, we first recall the expression for the anisotropic stress given in Ref. [13],

$$\pi_{ij}(\tau) = -4\bar{\rho}_\nu(\tau)\mathcal{H}^2 \int_0^\tau K(\tau-t)h'_{ij}(t)dt, \quad (3.6)$$

where K is the kernel defined as

$$\begin{aligned} K(\tau) &\equiv \frac{1}{16} \int_{-1}^1 dx (1-x^2)^2 e^{ix\tau}, \\ &= -\frac{\sin \tau}{\tau^3} - \frac{3 \cos \tau}{\tau^4} + \frac{3 \sin \tau}{\tau^5}. \end{aligned} \quad (3.7)$$

and $\bar{\rho}_\nu$ is the unperturbed neutrino energy density. To continue we then use Eq. (3.6) in Eq. (2.11). This gives the integro-differential equation for $h_{ij}(\tau)$ firstly derived in Ref. [13] and popularised by Ref. [8]

$$h''(\tau) + \frac{4(2+\tau)}{\tau(4+\tau)} h'(\tau) + k^2 h(\tau) = -24f_\nu(\tau) \left[\frac{4(2+\tau)}{\tau(4+\tau)} \right]^2 \int_0^\tau K(\tau-t)h'(t)dt. \quad (3.8)$$

This is the governing equation for linear tensor perturbations in a flat universe filled with radiation and pressureless matter, without a cosmological constant, and including a source term due to anisotropic stress, where $f_\nu = \bar{\rho}_\nu/\bar{\rho}$.

2. Radiation only with anisotropic stress

For a radiation only universe Eq. (3.8) reduces to

$$h''_r(\tau) + \frac{2}{\tau} h'_r(\tau) + k^2 h_r(\tau) = -24f_\nu(\tau) \left[\frac{4}{\tau^2} \right] \int_0^\tau K(\tau-t)h'_r(t)dt. \quad (3.9)$$

We proceed to use the method from [15] to get the solution for the first order h sourced by free-streaming neutrinos to compare with the analytic result Eq. (3.4). This gives

$$h_{r(1)}(\tau) = \left(-\frac{i}{k} \right) \left(\frac{e^{ik\tau - f_\nu(0)\tau}}{\tau} \right), \quad (3.10)$$

which is less than 1% away from the analytic solution without anisotropic stress.

IV. ANALYTICAL SOLUTIONS FOR THE TENSOR PERTURBATIONS

In this section, we will derive an approximate analytical solution to the governing equation Eq. (3.2) valid in the *sub-horizon* case, $k \gg \mathcal{H}$. We begin by recalling the method of Ref. [14] as applicable to a single second order differential equation, having a small parameter. Here, the small parameter is the co-moving inverse wave-number, k^{-1} .

As described in Ref. [15], the method consists of finding an approximation for h of the form

$$h(\tau) = \exp \left[\sum_{s=0}^{\infty} \int k^{-s+1} \omega_s(\tau) d\tau \right], \quad (4.1)$$

and for convenience, we write

$$\omega = \sum_{s=0}^{\infty} k^{-s+1} \omega_s(\tau), \quad (4.2)$$

where ω depends on both τ and k , and we will regard k as a fixed parameter. We then have

$$\begin{aligned} h' &= \omega h, \\ \text{and} \quad h'' &= (\omega' + \omega^2) h. \end{aligned} \tag{4.3}$$

A. Approximating perfect fluid tensor perturbations

Using the approximation of Eq. (4.1) in our governing equation Eq. (3.2), and dividing through by h , we get the ‘‘characteristic’’ equation from which we will derive all orders of our approximation,

$$(\omega' + \omega^2) + \frac{4(2 + \tau)}{\tau(4 + \tau)}\omega + k^2 = 0. \tag{4.4}$$

We can now substitute Eq. (4.2) into Eq. (4.4) and equate coefficients of like powers of the inverse wave-number, k^{-1} . The calculation is similar to that set out in a Bessel type differential equation in Ref. [15]. It can also be carried out using the *Mathematica* notebook available online at Ref. [16].

We can form successive order s_{\max} approximations

$$h_{(s_{\max})} = \exp \left[\sum_{s=0}^{s_{\max}} \int k^{-s+1} \omega_s(\tau) d\tau \right]. \tag{4.5}$$

We find that $h_{(s_{\max})}$ has complex values. Taking the real and imaginary parts of $h_{(s_{\max})}$ provides approximations for two independent solutions of Eq. (3.2).

For clarity, we should point out that, in this paper, when we describe an approximation as being of a particular order, we are not referring to the order of the perturbation theory (as described in, for example, Ref. [19]). We use the term order in this context to refer to the value of s_{\max} in the approximation of Eq. (4.5). We only use expressions of first order in perturbation theory, and, to minimise confusion, we consistently describe these as being of linear order.

The largest value of s_{\max} we shall use is $s_{\max} = 3$. This is because trial against numerical solutions² shows that larger choices of s_{\max} do not uniformly improve the approximation for all sub-horizon values of τ .

This third order approximation is to take any linear combination of the real and imaginary parts of

$$h_{(3)}(\tau) = \frac{1}{\tau(4 + \tau)} \left(\frac{4 + \tau}{\tau} \right)^{i/4k} \exp \left[ik\tau + \frac{1}{2k^2\tau(4 + \tau)} \right]. \tag{4.6}$$

Recall, as set out following Eq. (2.3), that τ and k have been normalised in terms of $\sqrt{2}/\mathcal{H}_{\text{eq}}$ and are therefore dimensionless numbers.

We want to compare our approximations with numerical solutions.³ Figure 3 shows the $h_{(3)}$ approximation for wave-number $k = 10\mathcal{H}_{\text{eq}}/\sqrt{2}$, plotted against the corresponding numerical solution.

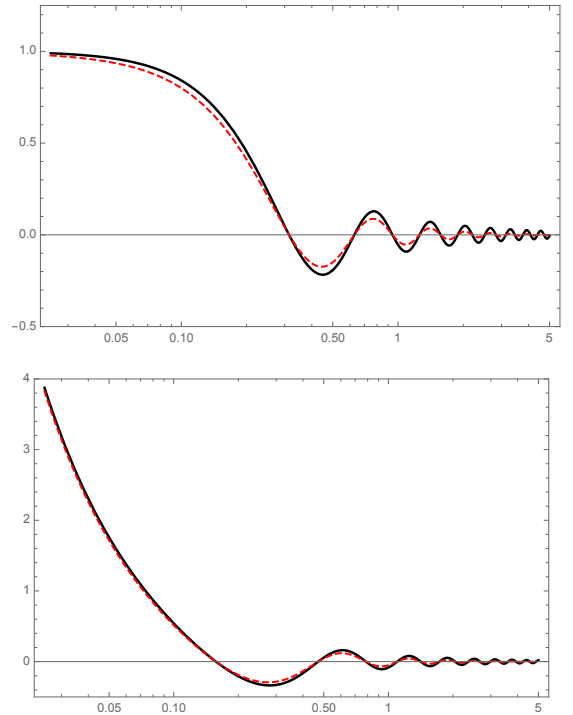


FIG. 2: *Upper panel:* Real components of the analytical and approximate solution for linear tensor perturbations in a flat radiation-only universe without (solid black line red dashed line) and with the effect of free streaming neutrinos anisotropic stress with $f_\nu(0) = 0.5$ (red dashed line), as set out in Eqs. (3.4) and (3.10). *Lower panel:* Imaginary components of Eqs. (3.4) and (3.10). The $k\tau$ axis is logarithmic.

² In Section VII of Ref. [15] we set out a method for estimating which order approximation is the most accurate for a given value of τ without employing numerical solutions.

³ As usual, our numerical solutions are derived from initial conditions. In Ref. [15] we had to use final conditions to manage a particular numerical instability.

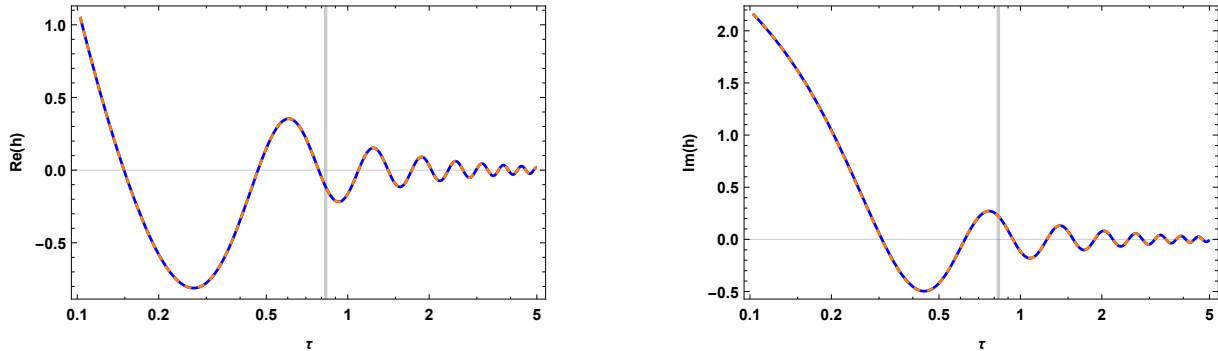


FIG. 3: The real and imaginary parts of the approximate third order solution for a perfect fluid given by Eq. (4.6) (solid blue line) and the numerical solution (dashed orange line) for Eq. (3.2) with $k = 10\mathcal{H}_{\text{eq}}/\sqrt{2}$. The horizontal axes show τ in units of τ_r , the conformal time of recombination, calculated using Ref. [3]. The curves are plotted for values of τ after horizon-crossing. The solid vertical line corresponds to radiation-matter equality, as defined by Eq. (2.4).

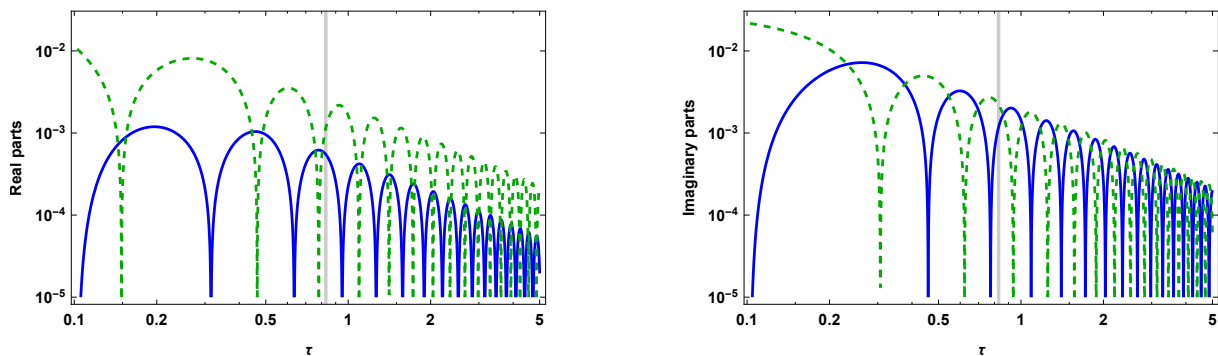


FIG. 4: The solid lines show the absolute errors in the approximation of Figure 3 as $|f_{(3)}(\tau) - f(\tau)|$, where $f_{(3)}$ is the real or imaginary part, as appropriate, of $h_{(3)}$ from Eq. (4.6) and f is the real or imaginary relevant part of the numerical solution for a perfect fluid. For comparison, the dashed line shows $|1\% \times f(\tau)|$. Downward spikes in the lines represent points where the value becomes zero. The blue solid line being below or level with the green dashed line indicates an error of less than or equal to 1%. See the text for further explanation.

We want now to quantify the error in the approximation $h_{(3)}$. One way to try to do this would be to take the numerical solution h and calculate the ratio $|(h_{(3)} - h)/h|$. However, this runs into a difficulty. Since h is oscillating and repeatedly takes zero values, unless there is no error at all at these zeros, the ratio $|(h_{(3)} - h)/h|$ will repeatedly become infinite.

We therefore adapt our approach in order to avoid this problem. Broadly speaking, we estimate the typical error compared with the amplitude of oscillation. To do this we first decide a target degree of accuracy, 1% say. We then compare a plot of the error $|h_{(3)} - h|$ with a plot of the target accuracy, here $1\% \cdot |h|$. Both plots will usually spike repeatedly downwards towards zero. We consider that the approximation is accurate to within 1% if, spikes when $h = 0$ aside, $|h_{(3)} - h| \leq 1\% \cdot |h|$. This will show on the graph as the plot of $|h_{(3)} - h|$ being level with, or below, the plot of $1\% \cdot |h|$ (except near $h = 0$ spikes).

As shown in Figure 4, the $h_{(3)}$ approximation is accurate to within 1%, or better from horizon-crossing onwards ($\tau \geq \tau_k$). In fact, this degree of accuracy applies for wave-numbers $k \gtrsim 9\mathcal{H}_{\text{eq}}/\sqrt{2} \sim 0.07 a_0 \text{ Mpc}^{-1}$. Using Eq. (2.7), this corresponds to actual present day distances of 17 Mpc.

The second order and first order approximations constructed by our method will also be of use in the next section, and we set them out here. The second order approximation is to take any linear combinations of the real and imaginary

parts of

$$h_{(2)}(\tau) = \frac{1}{\tau(4+\tau)} \left(\frac{4+\tau}{\tau} \right)^{i/4k} \exp[ik\tau]. \quad (4.7)$$

For use in Section V, we also write this more explicitly as

$$h_{(2)}(\tau) = \frac{B_s \sin \left(k\tau + \frac{1}{4k} \ln \left(1 + \frac{4}{\tau} \right) \right) + B_c \cos \left(k\tau + \frac{1}{4k} \ln \left(1 + \frac{4}{\tau} \right) \right)}{\tau(\tau+4)}, \quad (4.8)$$

with B_s and B_c real constants. This second order approximation is accurate to within 1%, or better, from horizon-crossing onwards, when we have $k \gtrsim 17\mathcal{H}_{\text{eq}}/\sqrt{2} \sim 0.12 a_0 \text{ Mpc}^{-1}$.

The first order, or leading order, approximation — as set out in [11] — is to take any linear combination of the real and imaginary parts of

$$h_{(1)}(\tau) = \frac{1}{\tau(4+\tau)} \exp[ik\tau] \propto \frac{\exp[ik\tau]}{a(\tau)} = \frac{\cos(k\tau) + i \sin(k\tau)}{a(\tau)}, \quad (4.9)$$

which is accurate to 1%, or better, from horizon-crossing onwards, when we have $k \gtrsim 120\mathcal{H}_{\text{eq}}/\sqrt{2} \sim 0.87 a_0 \text{ Mpc}^{-1}$.

B. Approximating tensor perturbations with anisotropic stress

In this section, we compute an approximate analytical solution to the governing equation Eq. (3.8). The fraction of the total energy density in neutrinos is [8]

$$f_\nu(\tau) = \frac{\Omega(a_0/a)^4}{\Omega_m(a_0/a)^3 + (\Omega_\gamma + \Omega_\nu)(a_0/a)^4} = \frac{f_\nu(0)}{1+\tau}, \quad (4.10)$$

We follow the method described in Ref. [15] along with (3.7) and (4.10) to get an approximate solution to Eq. (3.8). The third order approximation is to take any linear combination of the real and imaginary parts of

$$\begin{aligned} h_{(3)}(\tau) = & \left(-\frac{i}{k} - \frac{2(2+\tau)}{k^2\tau(4+\tau)} + \frac{i[16f_\nu(0)(2+\tau)^2 + 5(16+28\tau+15\tau^2+3\tau^3)]}{5k^3\tau^2(1+\tau)(4+\tau)^2} \right) \\ & \times \tau^{-1+(i/k)\alpha} (1+\tau)^{(i/k)\beta} (4+\tau)^{-1+(i/k)\gamma} \\ & \times \exp \left[ik\tau - f_\nu(0)\tau - \frac{2i[-15(2+\tau) + 4f_\nu(0)(6+\tau)]}{15k\tau(4+\tau)} + \frac{16f_\nu(0)(2+\tau)^2 + 5(16+28\tau+15\tau^2+3\tau^3)}{10k^2\tau^2(1+\tau)(4+\tau)^2} \right]. \end{aligned} \quad (4.11)$$

where

$$\alpha = \frac{5+8f_\nu(0)}{20}, \quad \beta = \frac{16}{45}f_\nu(0), \quad \text{and} \quad \gamma = \frac{45+8f_\nu(0)}{180}. \quad (4.12)$$

V. MODELLING PRIMORDIAL GRAVITATIONAL WAVES

In this section, we model the propagation of primordial gravitational waves from early times when the waves are super-horizon, through to later times when they are sub-horizon. We do this by matching an approximate solution for early times with a different one for late times. This gives us a solution valid for all times in the radiation-matter model, not just when the waves are sub-horizon.

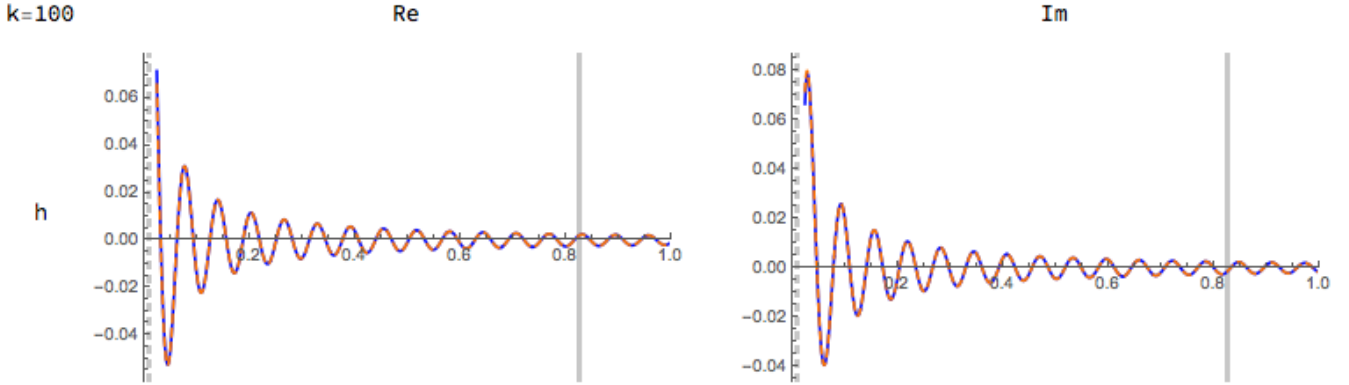


FIG. 5: The real and imaginary parts of the approximate third order solution with free neutrino anisotropic stress given by Eq. (4.11) (solid blue line) and the numerical solution (dashed orange line) for Eq. (3.8) with $k = 100\mathcal{H}_{\text{eq}}/\sqrt{2}$ and $f_\nu(0) = 0.40523$. The curves are plotted for values of τ after horizon-crossing. The solid vertical line corresponds to radiation-matter equality, as defined by Eq. (2.4).

For early times, we use the radiation-only solution, Eq. (3.4), while for late times we use the previous section's approximate solution $h_{(2)}$ from Eq. (4.8). We choose the time at which we match these solutions to be $\tau = 1/k$. We note from Eq. (3.5) that for relevant values of k , the matching time $\tau = 1/k$ will be close to the horizon-crossing time τ_k . The form of the resulting equations will, however, be much simpler than if we had done the matching at the horizon-crossing time itself.

The derivation of the approximations set out in the previous section depended on the sub-horizon assumption, $k \ll \mathcal{H}$. However, below we show that, for $k \gtrsim 4.5\mathcal{H}_{\text{eq}}/\sqrt{2}$, our matching approach gives an approximation, h_{rm} , which is accurate to 1%, or better, through the whole radiation-matter epoch. We use the second order solution $h_{(2)}$ in the matching because trial and error shows it is the order of approximate solution which works to within 1% for the widest range of wave-numbers.

From Eq. (3.4), we have that the early time solution is

$$h_r(\tau) = A_s \frac{\sin(k\tau)}{k\tau} + A_c \frac{\cos(k\tau)}{k\tau}. \quad (5.1)$$

As discussed above following Eq. (3.4), for gravitational waves with primordial origin, we can set $A_c = 0$. We therefore take

$$h_r(\tau) = \frac{\sin(k\tau)}{k\tau} \quad (5.2)$$

to be our solution for $\tau \leq 1/k$.

From Eq. (4.8), we have our solution for $\tau \geq 1/k$ as

$$h_{(2)}(\tau) = \frac{B_s \sin(\lambda(k, \tau)) + B_c \cos(\lambda(k, \tau))}{\tau(\tau + 4)}, \quad (5.3)$$

where we have written

$$\lambda(k, \tau) = k\tau + \frac{1}{4k} \ln \left(1 + \frac{4}{\tau} \right). \quad (5.4)$$

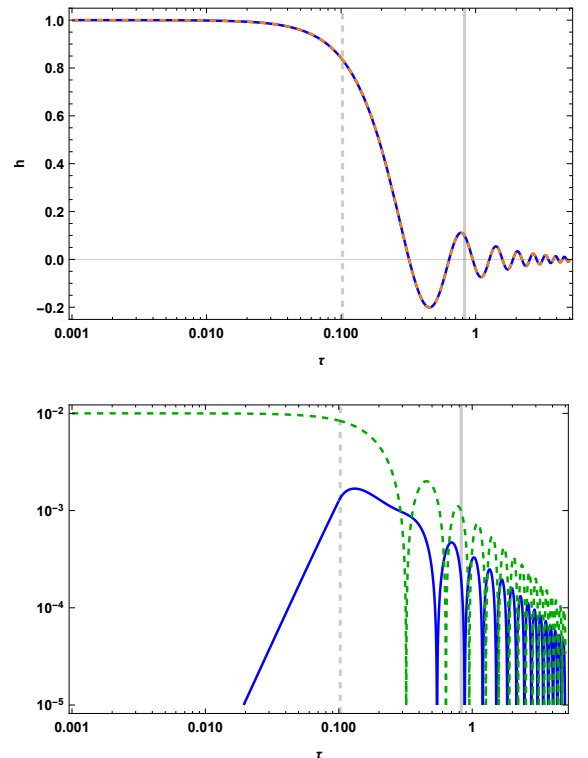


FIG. 6: *Upper panel:* The approximate solution, h_{rm} , of Eq. (5.5) (solid blue line) and the numerical solution for a perfect fluid (dashed orange line) for Eq. (3.2) with $k = 10\mathcal{H}_{\text{eq}}/\sqrt{2}$. *Lower panel:* The error in the matched solution (solid blue line) plotted against 1% of the numerical solution (dashed green line). *In both panels:* The vertical dashed line is horizon-crossing, $\tau_{k=10} \approx 0.102$, which is very close to the matching point, $\tau = 0.1$. The solid vertical line is radiation-matter equality.

We then need to choose the real constants B_s and B_c in Eq. (5.3) to be such that h_{rm} and h'_{rm} are continuous. In other words, we ensure the values of the two functions and the values of their first τ derivatives each match at $\tau = 1/k$. The calculation is set out in the Appendix. From Eq. (A10), we have the resulting matching approximation

$$h_{\text{rm}}(\tau) = \begin{cases} \frac{\sin(k\tau)}{k\tau} & \text{if } \tau \leq \frac{1}{k} \\ \frac{4k+1}{4k^3\tau(4+\tau)} \left[4k \sin(k\tau + L(k, \tau)) + \mu \sin(k\tau + L(k, \tau) - 1) \right] & \text{if } \tau \geq \frac{1}{k}, \end{cases} \quad (5.5)$$

where

$$L(k, \tau) = \frac{1}{4k} \ln \left(\frac{1 + 4\tau^{-1}}{1 + 4k} \right) \quad \text{and} \quad \mu = \sin(1) + \cos(1) = 1.38177\dots \quad (5.6)$$

This is our approximate analytical solution to Eq. (3.2), the governing equation for tensor perturbations (gravitational waves) in a flat radiation–matter universe. As we now show, it is a good approximation both sub–horizon ($\tau \lesssim 1/k$) and super–horizon ($\tau \gtrsim 1/k$) for wave–numbers k over a wide range of values relevant for structure formation in the Universe.

Figure 6 shows this matched solution, h_{rm} , for $k = 10\mathcal{H}_{\text{eq}}/\sqrt{2}$ in its upper panel and in the lower panel plots the error using the approach also used in Figure 4. The lower panel shows that the error is consistently less than 1%, both before and after horizon–crossing. We found that h_{rm} has errors of 1%, or better for all τ , when we $k \gtrsim 4.5\mathcal{H}_{\text{eq}}/\sqrt{2} = 0.033 a_0 \text{ Mpc}^{-1}$.

Using Eq. (2.7), this corresponds to h_{rm} meeting our 1% accuracy test for all times, when we consider inverse wave–numbers with actual present day values of less than, or equal to, around 35 Mpc. We can also express this in multipoles, as used in CMB calculations, via the broad correspondence — see for example Refs. [11, 20, 21] — that a multipole, l , receives its main contributions from present day physical wave–numbers $k_{\text{ph}} \simeq cH_0 l$. Using this rule, our range of 1% accuracy, $k \gtrsim 4.5\mathcal{H}_{\text{eq}}/\sqrt{2}$, broadly corresponds to multipoles $l \gtrsim 120$.

We found that matching using $h_{(1)}$ of Eq. (4.9), in place of $h_{(2)}$, obtains errors of 1%, or better for all τ , only when we have $k \gtrsim 180\mathcal{H}_{\text{eq}}/\sqrt{2} = 1.3 a_0 \text{ Mpc}^{-1}$. That corresponds to actual present day inverse wave–numbers of less, or equal to, around than 0.9 Mpc, and, broadly, to multipoles $l \gtrsim 5000$.

In the Introduction, we referred to the WKB solutions of Refs. [6, 9], Ref. [10] and Ref. [11]. These aim to derive approximations for primordial gravitational waves. We now compare these with our approximation — not restricting our attention only to the perfect fluid case but considering the anisotropic stress due to free–streaming neutrinos as well like Refs. [9–11].

Turning first to the WKB approximation of Ref. [11], we note that this is the same as our leading order approximation $h_{(1)}$ of Eq. (4.9). For primordial gravitational waves, along the lines discussed following Eq. (3.4), we are interested in only the imaginary, sine, part of Eq. (4.9), which is proportional to

$$h_{(1),s} = \frac{a_{\text{eq}} \sin(k\tau)}{k a(\tau)} = \frac{4 \sin(k\tau)}{k\tau(4+\tau)}, \quad (5.7)$$

where we have chosen the constant of proportionality so that $h_{(1),s}(0) = 1$. Figure 7 shows that, for $k = 10\mathcal{H}_{\text{eq}}/\sqrt{2}$, this gives errors of around 10%.

References [6, 9] presented another less straightforward form of WKB approximation. Figures in those papers show that, for $k \approx 16.4\mathcal{H}_{\text{eq}}/\sqrt{2}$ in Fig. 1 of Ref. [6], and for $k \approx 12.1\mathcal{H}_{\text{eq}}/\sqrt{2}$ in Fig. 2 of Ref. [9], there are errors of around 10%, or greater. Their figures also show that alternative simpler approximations — using a radiation–only solution, a matter–only solution, or the two matched together at $\tau = \tau_{\text{eq}}$ in a “sudden approximation” — are all less accurate than the WKB approximation of Refs. [6, 9], and so also much less accurate than our approximation h_{rm} , given in Eq. (5.5).

Our calculations suggest that the best approximation we have found in the literature for sub–horizon primordial gravitational waves is the WKB solution explored in passing in Ref. [10]. That approximation is constructed for only one of the two independent solutions of the governing equation Eq. (3.2). As can be seen from Figure 4, typically one of a pair of approximate WKB solutions will be better than the other. For $k = 10\mathcal{H}_{\text{eq}}/\sqrt{2}$, and for sub–horizon values of τ , the approximation of Ref. [10] is accurate to within about 0.8%, which compares with the accuracies for the two approximations of Figure 4 of around 0.25% (real part) and 1% (imaginary part). When started outside the horizon, Ref. [10]’s approximation becomes considerably less accurate than our matching approximation, h_{rm} .

The Bessel function approach of Ref. [12] also approximates primordial gravitational waves. As indicated in Section I, a comparison with numerical solutions shows that many terms are needed to derive accurate approximations.

VI. CONCLUSION

In this work we have derived new analytic solutions to the gravitational wave or tensor evolution equation at linear order in cosmological perturbation theory, using the method presented in Ref. [15] and including neutrino anisotropic stress. The solutions depend on time, wavenumber, and the ratio of the neutrino background energy density and the total energy density at $\tau = 0$, $f_\nu(0)$, which allows to vary the damping of the gravitational waves due to the neutrino anisotropic stress.

We show how the method of Ref. [15] can be applied to an integro-differential equation, and our solutions present a simple way to analyse the evolution of the tensor perturbations in the presence of anisotropic stress. The analytic solutions save computational time compared to solving the equations numerically, for example if we are interested in a wide range of different parameter values f_ν , the ratio of neutrino to total background energy density. We have compared our analytical approximation to numerical solutions with anisotropic stress and find that the difference between them is within 1%.

A simple example will illustrate the usefulness of analytical solutions even in this day and age. In second order cosmological perturbation theory, the governing equations include terms of the form $h_{ij}h^{ij}$. For example it has been shown in Ref. [22] that different forms of the curvature perturbation at second order differ by terms proportional to $h_{ij}h^{ij}$. To relate this to the expressions derived in the sections above, we can use that for a gravitational wave travelling in the z -direction, for example,

$$h_{ij}h^{ij} = 2 \left[(h^\times)^2 + (h^+)^2 \right], \quad (6.1)$$

where h^\times and h^+ are the two independent polarisations of the gravitational waves defined in Eq. (2.9). Then substituting in the solutions of the model we are interested in, we get an expression of how much the different curvature perturbations disagree in terms of, say, the wavenumber and the neutrino-radiation ratio f_ν . We shall return to these issues in future work.

Acknowledgements

The authors are grateful to Pedro Carrilho for useful discussions. KAM is supported, in part, by STFC grant ST/J001546/1. JLF acknowledges support of a studentship funded by Queen Mary University of London as well as CONACYT grant No. 603085.

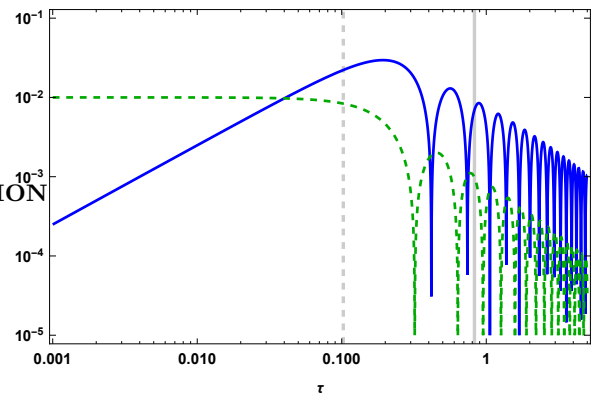


FIG. 7: As for the lower panel of Figure 6, but using the leading order approximation, $h_{(1),s}$ of Eq. (5.7), instead of h_{rm} .

-
- [1] B. P. Abbott, R. Abbott, T. D. Abbott, M. R. Abernathy, F. Acernese, K. Ackley, C. Adams, T. Adams, P. Addesso, R. X. Adhikari, and et al., Physical Review Letters **116**, 061102 (2016), arXiv:1602.03837 [gr-qc] .
 - [2] P. A. R. Ade, N. Aghanim, Z. Ahmed, R. W. Aikin, K. D. Alexander, M. Arnaud, J. Aumont, C. Baccigalupi, A. J. Banday, D. Barkats, and et al. ((BICEP2/Keck and Planck Collaborations)), Phys. Rev. Lett. **114**, 101301 (2015), arXiv:1502.00612 [astro-ph.CO] .
 - [3] Planck Collaboration, P. A. R. Ade, N. Aghanim, M. Arnaud, M. Ashdown, J. Aumont, C. Baccigalupi, A. J. Banday, R. B. Barreiro, J. G. Bartlett, and et al., ArXiv e-prints (2015), arXiv:1502.01589 [astro-ph.CO] .
 - [4] M. S. Turner, M. White, and J. E. Lidsey, Phys. Rev. D **48**, 4613 (1993), arXiv:astro-ph/9306029 .
 - [5] B. Allen and S. Koranda, Phys. Rev. D **50**, 3713 (1994), arXiv:astro-ph/9404068 .
 - [6] K.-W. Ng and A. D. Speliotopoulos, Phys. Rev. D **52**, 2112 (1995), arXiv:astro-ph/9405043 .
 - [7] Y. Wang, Phys. Rev. D **53**, 639 (1996), arXiv:astro-ph/9501116 .

- [8] S. Weinberg, Phys. Rev. D **69**, 023503 (2004), arXiv:astro-ph/0306304 [astro-ph] .
- [9] J. R. Pritchard and M. Kamionkowski, Annals of Physics **318**, 2 (2005), arXiv:astro-ph/0412581 .
- [10] S. Bashinsky, ArXiv Astrophysics e-prints (2005), arXiv:astro-ph/0505502 .
- [11] S. Weinberg, *Cosmology, by Steven Weinberg. ISBN 978-0-19-852682-7. Published by Oxford University Press, Oxford, UK, 2008.* (Oxford University Press, 2008).
- [12] B. A. Stefanek and W. W. Repko, Phys. Rev. D **88**, 083536 (2013), arXiv:1207.7285 [hep-ph] .
- [13] A. K. Rebhan and D. J. Schwarz, Phys. Rev. D **50**, 2541 (1994).
- [14] S. F. Feshchenko, N. I. Shkil, and L. D. Nikolenko, *Asymptotic methods in the theory of linear differential equations, S.F. Feshchenko, N.I. Shkil, and L.D. Nikolenko. Translated by Scripta Technica* (American Elsevier Pub. Co New York, 1966) pp. xvi, 270 p., translated for the National Aeronautics and Space Administration by John F. Holman and Co. Inc. NASw-1495 20546, available at https://archive.org/details/nasa_techdoc_19670019838 online.
- [15] A. J. Wren and K. A. Malik, Phys. Rev. **D95**, 083526 (2017), arXiv:1603.07577 [gr-qc] .
- [16] A. J. Wren and K. A. Malik, “Mathematica notebooks for *TBC - THIS PAPER*,” (2016), available at TBC .
- [17] T. Padmanabhan, in *Graduate School in Astronomy: X*, American Institute of Physics Conference Series, Vol. 843, edited by S. Daffon, J. Alcaniz, E. Telles, and R. de la Reza (2006) pp. 111–166, arXiv:astro-ph/0602117 .
- [18] E. L. Wright, PASP **118**, 1711 (2006), arXiv:astro-ph/0609593 .
- [19] K. A. Malik and D. Wands, Phys. Rep. **475**, 1 (2009), arXiv:0809.4944 [astro-ph] .
- [20] B. Ryden, *Introduction to cosmology / Barbara Ryden. San Francisco, CA, USA: Addison Wesley, ISBN 0-8053-8912-1, 2003, IX + 244 pp.* (Addison Wesley, 2003).
- [21] D. H. Lyth and A. R. Liddle, *The Primordial Density Perturbation, by David H. Lyth, Andrew R. Liddle, Cambridge, UK: Cambridge University Press, 2009* (2009).
- [22] P. Carrilho and K. A. Malik, J. Cosmology Astropart. Phys. **2**, 021 (2016), arXiv:1507.06922 [astro-ph.CO] .

Appendix A: Calculation of the matching conditions for approximating primordial gravitational waves

In this appendix, we calculate the matching conditions needed to obtain the solution in Eq. (5.5) of Section V. We start by matching the values of the functions h_r of Eq. (5.2) and $h_{(2)}$ of 5.3 at the conformal time $\tau = 1/k$. This gives

$$\begin{aligned} \sin(1) &= \frac{B_s \sin\left(\lambda\left(k, \frac{1}{k}\right)\right) + B_c \cos\left(\lambda\left(k, \frac{1}{k}\right)\right)}{\frac{1}{k}\left(\frac{1}{k} + 4\right)} \\ &= \frac{k^2}{4k + 1} \left\{ B_s \sin\left(\lambda\left(k, \frac{1}{k}\right)\right) + B_c \cos\left(\lambda\left(k, \frac{1}{k}\right)\right) \right\}, \end{aligned} \quad (\text{A1})$$

where

$$\lambda\left(k, \frac{1}{k}\right) = 1 + \frac{1}{4k} \ln(1 + 4k). \quad (\text{A2})$$

Note that

$$\left. \frac{\partial(\lambda(k, \tau))}{\partial \tau} \right|_{\tau=\frac{1}{k}} = k - \frac{1}{k\tau^2 + 4k\tau} \Big|_{\tau=\frac{1}{k}} = k - \frac{k}{4k + 1} = \frac{4k^2}{4k + 1}, \quad (\text{A3})$$

and

$$\left. \frac{\partial\left(\frac{1}{\tau(\tau+4)}\right)}{\partial \tau} \right|_{\tau=\frac{1}{k}} = -\frac{2(\tau+2)}{\tau^2(\tau+4)^2} \Big|_{\tau=\frac{1}{k}} = -\frac{2k^3(2k+1)}{(4k+1)^2}. \quad (\text{A4})$$

Using Eqs. A3 and A4 to calculate $h'_{(2)}(1/k)$, we match the first derivatives of with respect to τ of h_r and $h_{(2)}$ at $\tau = 1/k$ to get

$$\begin{aligned} k \cos(1) - k \sin(1) &= \frac{4k^4}{(4k+1)^2} \left\{ B_s \cos\left(\lambda\left(k, \frac{1}{k}\right)\right) - B_c \sin\left(\lambda\left(k, \frac{1}{k}\right)\right) \right\} \\ &\quad - \frac{2k^3(2k+1)}{(4k+1)^2} \left\{ B_s \sin\left(\lambda\left(k, \frac{1}{k}\right)\right) + B_c \cos\left(\lambda\left(k, \frac{1}{k}\right)\right) \right\}. \end{aligned} \quad (\text{A5})$$

We can solve Eqs. A1 and A5 simultaneously to find

$$\begin{aligned}
B_s &= \frac{4k+1}{4k^3} \left\{ 4k \left[\cos(1) \cos \left(\lambda \left(k, \frac{1}{k} \right) \right) + \sin(1) \sin \left(\lambda \left(k, \frac{1}{k} \right) \right) \right] + [\sin(1) + \cos(1)] \cos \left(\lambda \left(k, \frac{1}{k} \right) \right) \right\} \\
&= \frac{4k+1}{4k^3} \left\{ 4k \cos \left(1 - \lambda \left(k, \frac{1}{k} \right) \right) + [\sin(1) + \cos(1)] \cos \left(\lambda \left(k, \frac{1}{k} \right) \right) \right\} \\
&= \frac{4k+1}{4k^3} \left\{ 4k \cos \left(\frac{1}{4k} \ln(1+4k) \right) + [\sin(1) + \cos(1)] \cos \left(1 + \frac{1}{4k} \ln(1+4k) \right) \right\}
\end{aligned} \tag{A6}$$

and

$$\begin{aligned}
B_c &= \frac{4k+1}{4k^3} \left\{ 4k \left[\sin(1) \cos \left(\lambda \left(k, \frac{1}{k} \right) \right) - \cos(1) \sin \left(\lambda \left(k, \frac{1}{k} \right) \right) \right] - [\sin(1) + \cos(1)] \sin \left(\lambda \left(k, \frac{1}{k} \right) \right) \right\} \\
&= \frac{4k+1}{4k^3} \left\{ 4k \sin \left(1 - \lambda \left(k, \frac{1}{k} \right) \right) - [\sin(1) + \cos(1)] \sin \left(\lambda \left(k, \frac{1}{k} \right) \right) \right\} \\
&= \frac{4k+1}{4k^3} \left\{ -4k \sin \left(\frac{1}{4k} \ln(1+4k) \right) - [\sin(1) + \cos(1)] \sin \left(1 + \frac{1}{4k} \ln(1+4k) \right) \right\},
\end{aligned} \tag{A7}$$

where we recalled the definition of $\lambda(k, \tau)$ from Eq. (5.4). In going from the first to second lines of Eqs. A6 and A7, we have used standard trigonometric addition formulae.

From Eq. (5.3), this gives us

$$\begin{aligned}
h_{(2)}(\tau) &= \frac{4k+1}{4k^3\tau(4+\tau)} \left[4k \left\{ \cos \left(\frac{1}{4k} \ln(1+4k) \right) \sin(\lambda(k, t)) - \sin \left(\frac{1}{4k} \ln(1+4k) \right) \cos(\lambda(k, t)) \right\} \right. \\
&\quad \left. + [\sin(1) + \cos(1)] \left\{ \cos \left(1 + \frac{1}{4k} \ln(1+4k) \right) \sin(\lambda(k, t)) \right. \right. \\
&\quad \left. \left. - \sin \left(1 + \frac{1}{4k} \ln(1+4k) \right) \cos(\lambda(k, t)) \right\} \right]
\end{aligned} \tag{A8a}$$

$$= \frac{4k+1}{4k^3\tau(4+\tau)} \left[4k \sin(k\tau + L(k, t)) + [\sin(1) + \cos(1)] \sin(k\tau + L(k, t) - 1) \right], \tag{A8b}$$

where again we recalled the definition of $\lambda(k, \tau)$ from Eq. (5.4), and we have defined

$$L(k, \tau) = \frac{1}{4k} \ln \left(\frac{1+4\tau^{-1}}{1+4k} \right). \tag{A9}$$

We used standard trigonometric addition formulae to go from Eq. (A8a) to Eq. (A8b).

From Eq. (5.2) and Eq. (A8b), the matching approximation is therefore

$$h_{\text{rm}}(\tau) = \begin{cases} \frac{\sin(k\tau)}{k\tau} & \text{if } \tau \leq \frac{1}{k} \\ \frac{4k+1}{4k^3\tau(4+\tau)} \left[4k \sin(k\tau + L(k, t)) + \mu \sin(k\tau + L(k, \tau) - 1) \right] & \text{if } \tau \geq \frac{1}{k}, \end{cases} \tag{A10}$$

where $\mu = \sin(1) + \cos(1) = 1.38177\dots$

Appendix B: Calculation of the anisotropic stress solution

The method described in Ref. [15] works best for equations like

$$\mathbf{A}\mathbf{f}''(\tau) + \mathbf{C}\mathbf{f}'(\tau) + \mathbf{B}\mathbf{f}(\tau) = \mathbf{0}. \quad (\text{B1})$$

so we take Eq. (3.8) and write it as a system of ordinary second order differential equations to get⁴

$$\mathbf{A}\mathbf{X}''(\tau) + \mathbf{C}\mathbf{X}'(\tau) + \mathbf{B}\mathbf{X}(\tau) = \mathbf{0}. \quad (\text{B2})$$

where

$$\mathbf{X}(\tau) = \begin{bmatrix} x_1(\tau) \\ x_2(\tau) \end{bmatrix} = \begin{bmatrix} h(\tau) \\ h'(\tau) \end{bmatrix},$$

and

$$\mathbf{A} = \begin{bmatrix} 1 & 0 \\ 0 & 1 \end{bmatrix}, \quad \mathbf{C}(\tau) = \begin{bmatrix} 0 & -1 \\ 0 & f_2(\tau)/f_1(\tau) \end{bmatrix}, \quad \mathbf{B}(\tau) = \begin{bmatrix} 0 & 0 \\ f_4(\tau)/f_1(\tau) & f_3(\tau)/f_1(\tau) \end{bmatrix},$$

where we have defined

$$f_1(\tau) = -\frac{1}{96f_\nu(0)} \frac{\tau^2(1+\tau)(4+\tau)^2}{(2+\tau)^2}, \quad (\text{B3})$$

$$f_2(\tau) = -\frac{1}{96f_\nu(0)} \frac{\tau(4+\tau)\{32 + \tau(64 + \tau[36 + 7\tau])\}}{(2+\tau)^3}, \quad (\text{B4})$$

$$f_3(\tau) = -\frac{1}{96f_\nu(0)} \frac{32 + \tau\{80 + \tau[44 + 8\tau + k^2(1+\tau)(4+\tau)^2]\}}{(2+\tau)^2} - \frac{1}{15}, \quad (\text{B5})$$

$$f_4(\tau) = -\frac{1}{96f_\nu(0)} \frac{k^2\tau\{4 + \tau[16 + \tau(16 + 3\tau)]\}}{121569(2+\tau)^3}. \quad (\text{B6})$$

Following Ref. [15] we need to further decompose $\mathbf{B}(\tau) = \mathbf{B}_0(\tau) + \mathbf{B}_{-2}(\tau)k^2$ and those matrices are

$$\mathbf{B}_0(\tau) = \begin{bmatrix} 0 & 0 \\ 0 & b_0(\tau) \end{bmatrix}, \quad \text{and} \quad \mathbf{B}_{-2}(\tau) = \begin{bmatrix} 0 & 0 \\ b_{-2}(\tau) & 1 \end{bmatrix}.$$

where

$$b_0(\tau) = \frac{4\{8f_\nu(0)(2+\tau)^2 + 5(8 + \tau[20 + \tau(11 + 2\tau)])\}}{5\tau^2(1+\tau)(4+\tau)^2}, \quad (\text{B7})$$

$$b_{-2}(\tau) = \frac{2}{\tau} + \frac{1}{1+\tau} - \frac{2}{2+\tau} + \frac{2}{4+\tau}. \quad (\text{B8})$$

Finally, we use the *Double Power Series Method* in Ref. [16] to get Eqs. (3.10) and (4.11).

⁴ **Note.** We are neglecting the term $\int_0^\tau K'(\tau-t)h'(t)dt$ that arises from differentiating Eq. (3.8) because numerically the value is *negligible*.